JOURNAL OF MATERIALS SCIENCE 31 (1996) 6285–6292

The a.c. impedance response of concrete during early hydration

W.J. McCARTER
Department of Civil and Offshore Engineering, Heriot-Watt University, Edinburgh EH14 4AS, UK

The complex impedance response of fresh concrete was investigated over the frequency range 100 Hz–10 MHz, together with resistivity measurements on the interstitial water phase. The work corroborates and extends previous studies both in the range of concretes tested and modelling of the data. It is shown that the contained water-phase within the concrete exerts a considerable influence of the impedance response and, as such, is related to the type of cemetitious binder. When the bulk resistivity of the concrete is normalized by that of the contained water, a direct relationship exists between this value and the fractional water content of the concrete. Possibilities exist for the application of impedance spectroscopy techniques in the quality control of structural concrete.

1. Introduction and background

Since the first reported application of impedance spectroscopy to Portland cement paste [1], considerable effort has been directed by workers in using this technique for characterizing cement microstructure [2–20]. Considerable advances have now been made in the quantitative understanding of complex impedance plots and their dependence on microfabric features such as gel formation, capillary porosity, pore tortuosity and connectivity and distribution of water within the capillary pore network. Such developments have been undertaken on neat cement paste and mortar samples, with particular emphasis on the period after setting.

The complex impedance response of hardening cement paste (HCP) is characterized by a depressed (bulk) arc developing over the frequency range 5 kHz –15 MHz (approximately), together with a low-frequency spur. This spur is part of a much larger arc which develops at low frequencies and is attributed to polarization effects at the electrode/HCP interface region. While still in the liquid state (i.e. before setting), this bulk arc was only weakly developed [16] or not present [9, 14, 21, 22] and the response for plain cement pastes is dominated by the spur associated with electrode processes. It is only after setting that the high-frequency arc develops and is associated with the formation of a randomly orientated capillary pore network.

Because the bulk arc is not observed for cement pastes during the very early stages of hydration (i.e. before setting), work has, naturally, concentrated complex impedance measurements on the period after setting. However, this does not imply a dearth of electrical measurements on cement pastes, mortars or concretes prior to setting; on the contrary, this has been an area of interest since the 1920s [23–35]. Prime motivation of such work has been the application of electrical measurements for setting-time determination. Such measurements have been presented at either a single frequency or at several spot frequencies within a limited frequency range, typically 100 Hz –10 kHz. Furthermore, the macroscopic response of concrete to an alternating electrical field has been represented by a purely resistive model; little attention has been paid to the existence of possible bulk polarization phenomena resulting in a capacitive component to the measured impedance.

Lately, however, work has been undertaken on investigating both the in-phase and quadrature components of impedance [16, 17, 36–39] of cement pastes and mortars, in particular the variation of the individual components over the initial 24 h after mixing with water. The frequencies used in this work covered the range 20 Hz–7 MHz and have led to insights into mechanisms of cement hydration. High-frequency dielectric measurements (as opposed to complex impedance measurements), taken over the frequency range 1–300 MHz [40], have been presented for mortar samples during the initial 24 h. It must be emphasized that studies have been limited in (a) the range of mix proportions employed (and not related to industry standard concretes), and (b) the range of cementitious binders. Regarding the latter, in the design of concrete for durability, increasing use is being made of replacement materials, such as pulverized fuel ash (PFA) and ground granulated blast-furnace slag (GGBS).

It is only recently [22] that complex impedance measurements (Nyquist plots) have been presented on concretes (as opposed to mortars) prior to setting. These measurements have shown that even at this early stage in the hydration process, a bulk arc

0022–2461

develops and is strongly related to the volume fraction of aggregate within the concrete. As noted above, this arc is not observed in cement paste at such early stages.

This paper shows, in a more systematic way, the influence of cementitious binder and water content on the impedance response of fresh concrete. In addition to this, the electrical properties of the interstitial water phase within the concrete are examined and further interpretations of electrical data presented. Ascertaining the exact inter-relationship between the various phases within such a composite material could result in an effective quality control technique for structural concrete. Regarding such an application, many problems associated with concrete deterioration are as a result of poor quality control at the production stage; in addition, there is considerable advantage in undertaking remedial measures before the concrete sets.

2. Experimental procedure

2.1. Preliminaries

Concrete is a heterogeneous material comprising aggregate, cement and water mixed in varying proportions. The aggregate is further sub-divided into a coarse fraction and a fine fraction. The coarse aggregate fraction comprises a gradation of particles ranging from, approximately, 5–20 mm, whereas the fine fraction has particle sizes within the range 150 μm –5 mm. Cement particles, themselves, are of the order of 50 μm. When water is added to cement particles, a series of complex chemical reactions occurs which result in eventual setting and hardening of the cement paste. Initial hydrolysis results in the interstitial aqueous phase becoming saturated with respect to Ca^{2+} and OH^-, other ions such as Na^+, K^+ and SO_4^{2-} are also present. The bulk resistivity of aggregates used in concretes is, typically, in the range 10^2–10^6 Ωm [41,42] while that of Portland cement paste (before setting) is approximately 1 Ωm [22]. It could be concluded that, from an electrical point of view, concrete can be considered as non-conductive aggregate particles embedded in an ionically conducting cement paste matrix. Indeed, this argument could be taken one stage further by proposing that the cement paste itself could be considered as non-conductive cement grains surrounded by an ionically conducting, interstitial fluid phase.

2.2. Mix details

A series of tests was undertaken on a range of cementitious binders represented by ordinary Portland cement (OPC), sulphate-resisting Portland cement (SRPC), OPC with PFA at 30% replacement, and OPC with GGBS at 50% replacement. These materials conformed to current British Standards [43–46].

The coarse aggregate had a nominal maximum size of 20 mm and the fine aggregate conformed to Zone M [47]; a natural gravel aggregate was used throughout. A pan mixer was used and mixing time was kept constant at 1 min as measured from the initial addition of water. Prior to gauging, the constituents were dry mixed for approximately 30 s.

Full details of the mixes studied are presented in Table I and designed in accordance with Teychenne *et al.* [48]. The 28-day compressive strength [49] of these mixes, denoted F_{28}, is also presented in this table.

2.3. Electrical measurements

After mixing, the material was compacted in rigid, plastic cells. The internal dimensions of the test cells were 15 cm × 15 cm × 15 cm and considered large enough to obtain a representative, bulk impedance response (approximately 8 kg material). These dimensions also conformed to the British Standard cube size for strength tests on concretes [50]. Two opposite sides of the cell were fitted with 15 cm × 15 cm stainless steel electrodes (Type 304) with each electrode secured to the side of the cell by means of four stainless steel bolts; one bolt passed through the side of the cell which served as the point of electrical connection. Impedance measurements were taken using a Solartron 1260 impedance gain/phase analyser operating within the frequency range 100 Hz–10 MHz.

Data were obtained at 150 spot frequencies within this range using a logarithmic frequency sweep with the 1260 operating in voltage drive mode. Three samples were tested for each concrete mix in Table I. All tests were carried out at 20 ± 2 °C, 55%–60% RH. Individually screened, coaxial cables connected

TABLE I Concrete mixes used in the experimental programme. Note that binder refers to the total amount of cementitious material (i.e. cement + replacement). ND = not determined

Mix	Water–binder ratio	Free water content ($kg\,m^{-3}$)	Total aggregate content ($kg\,m^{-3}$)	Replacement	Cement	F_{28} (MPa)
1	0.38	135	1955	–	OPC	52
2	0.38	160	1790	PFA30%	OPC	47
3	0.44	180	1795	–	OPC	39
4	0.44	180	1795	GGBS50%	SRPC	37
5	0.44	180	1795	–	SRPC	38
6	0.44	185	1770	GGBS50%	OPC	39
7	0.47	150	1945	–	OPC	ND
8	0.50	140	1975	PFA30%	OPC	32
9	0.50	150	1930	PFA30%	OPC	32
10	0.56	215	1725	–	OPC	33

the sample to 1260 output terminals (Gen. Out; V(hi); V(lo); current in), these cables being coupled (and attached) at the stainless steel electrodes by means of crocodile clips (Gen. Out coupled with V(hi), and V(lo) coupled with current in). Cable outers were shorted as close as possible to the sample by means of a stainless steel rod. Lead and cell open- and short-circuit residual impedances were nulled from the incoming data at all test frequencies. All data were logged by computer (HP Vectra 486/66N) with impedance measurements being taken 30 min after mixing.

In addition to these bulk impedance measurements, conductivity measurements were taken on the interstitial fluid phase which was extracted from the sample using a vacuum filtration technique. This fluid was extracted from the respective concrete sample immediately after impedance measurements. The filtering system prevented cement particles from contaminating the extracted water. Fluid conductivity and temperature measurements were obtained using a Jenway 4020 conductivity meter and conductivity cell.

3. Results and discussion

3.1. Measurements on OPC concretes

Fig. 1 presents the impedance response for the four plain OPC concrete mixes with water–binder ratios ranging from 0.38 to 0.56 (the water–binder ratio, in the context of this paper, is defined as the mass of water in a mix divided by the mass of cementitious binder). It is immediately apparent that, unlike neat cement pastes during these early stages of hydration, a bulk arc develops in the complex plane and corroborates a previous study [22]. This was attributed to the time constant of the system being moved into an observable frequency range, as the inclusion of the low-conductivity aggregate phase increases the bulk resistance of the composite. The remnants of the spur associated with electrode effects are also visible on the right-hand side of the plots.

From the plots in Fig. 1, there was distortion of the bulk arc at frequencies in excess of 4 MHz. Although lead-inductive effects were nulled from the incoming data at all test frequencies, there must be residual effects which are still degrading the data at these higher frequencies, this is made more prominent due to the low impedance of the concrete sample. Fig. 1 also shows that there is no direct relationship between water–binder ratio and impedance behaviour; however, if the water content alone is considered, then an inverse relationship exists between measured impedance and the volume fraction of conductive water phase in the mix. The converse of this statement may also be appropriate as increasing the volume fraction of non-conductive aggregate phase results in a dilution effect, thereby increasing the system impedance.

It is also interesting to note that the resistivity, ρ_w, of the contained water phase (see Table II) increases from 0.58 Ωm to 0.64 Ωm as the water content is increased from, respectively, 135 kg m^{-3} to 215 kg m^{-3}; reduced ionic concentration within the water would account for this slight increase. Because the changes in impedance cannot be attributed to any marked changes in the ionic conductivity of the interstitial fluid then, for a given cementitious binder, the variations in impedance are almost entirely due to the reduced cross-sectional area available for conduction processes (or the increase in the volume fraction of non-conductive phase).

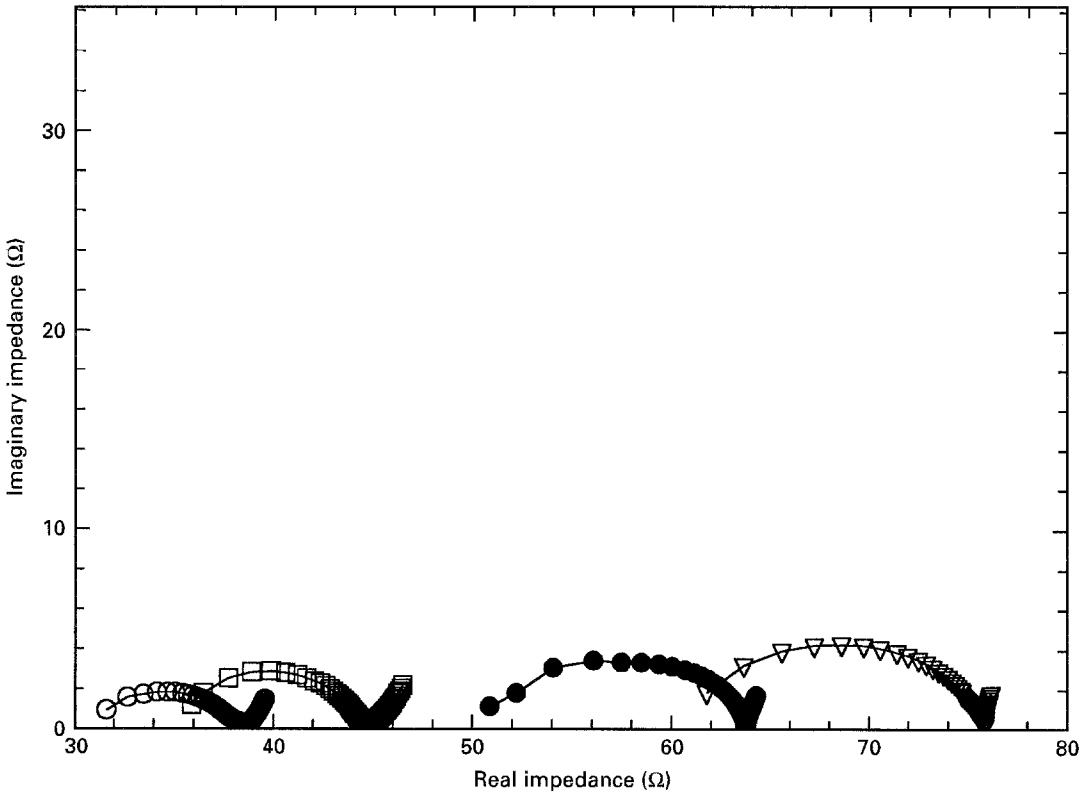

Figure 1 Complex impedance spectra for OPC concretes: (▽) Mix 1, water content 135 kg m^{-3}; (□) Mix 3, water content 180 kg m^{-3}; (●) Mix 7, water content 150 kg m^{-3}; (○) Mix 10, water content 215 kg m^{-3}.

TABLE II Summary of bulk resistivity measurements of concretes and interstitial water phase

Mix	ρ_{bulk} (Ω-m)	ρ_w (Ω-m)	ρ_w/ρ_{bulk} ($\times 10^{-2}$)
1	8.55	0.58	6.78
2	9.70	0.71	7.28
3	6.19	0.58	9.39
4	15.44	1.50	9.89
5	10.00	0.91	9.06
6	13.06	1.24	9.46
7	8.26	0.60	7.27
8	16.56	1.10	6.64
9	16.00	1.15	7.22
10	5.94	0.64	10.77

TABLE III Summary of model parameters of OPC concrete mixes

Mix	R_{bulk} (Ω)	Y_{bulk} (F)	n_{bulk}
1	76	1.21×10^{-7}	0.53
3	48	1.56×10^{-7}	0.55
7	64	1.37×10^{-7}	0.53
10	39	1.68×10^{-6}	0.42

As there was distortion at the high-frequency end of the arc, the data at frequencies below 3 MHz were used to estimate equivalent circuit parameters for the response namely the bulk resistance, R_{bulk}, and the constant phase element (CPE), $Q_{bulk}(= Y_{bulk}(j\omega)^n)$. This was undertaken using the software package EQUIVCRT [51]with the bulk arc modelled on a parallel ($R_{bulk}Q_{bulk}$) circuit and origin taken to lie on this arc at infinite frequency. This model is taken in preference to an $R_0(R_{bulk}Q_{bulk})$ circuit which has been used for HCP. In this model, R_0 represents the high-frequency intercept with the real axis – the so-called offset resistance [18]. There is debate over the offset resistance; it has been proposed that it is simply an artefact of the null-correction procedures, i.e. the inability completely to null-correct data for lead-inductive effects [19] at high frequencies; it has also been conjectured [17] that a smaller arc, at still higher frequencies, could exist which would take the response towards the origin. This smaller arc is attributed to growth of calcium silicate hydrate (C–S–H) into the water-filled capillary pores. In the liquid state, it is more likely to be the former, as no capillary pore structure exists.

On application of an electric field, the main current paths will follow a convoluted path around the aggregate inclusions as their resistivity is several orders of magnitude greater than that of the highly conductive interstitial water phase. There will, however, always be some current flow from the fluid phase through the aggregate and back to the fluid phase. At the point where current flows from the conductive phase to the resistive phase there will be an accumulation and diffusion of charges at and over this interface, and must give rise to an interfacial capacitive effect. The circuit elements obtained from this analysis are displayed in Table III for the plain OPC mixes. Interestingly, as the water content of the mix is reduced from 215 $kg\,m^{-3}$ to 180 $kg\,m^{-3}$, the coefficient of the CPE decreases by almost an order of magnitude; however, reducing the water content from 180 $kg\,m^{-3}$ to 135 $kg\,m^{-3}$ results in a much more gradual decrease in the CPE, with the impedance being dominated by the bulk resistance of the system.

3.2. Influence of cementitious binder

Consider now Fig. 2, in which the cementitious binder is altered (i.e. GGBS + SRPC; SRPC, and GGBS + OPC). It is clear from this figure that the cementitious binder, itself, exerts a pronounced influence on the impedance of the system. Water contents for this series of tests were held within a narrow range (180–185 $kg\,m^{-3}$), with the water–binder ratio constant. The volume fraction of aggregate phase is thus virtually the same for all mixes. When compared to the equivalent plain OPC concrete (i.e. mix 3), the increase in the impedance of the concrete containing SRPC is attributed solely to the increase in resistivity of the contained water phase (see Table II). This has increased from 0.58 Ωm to 0.91 Ωm. The SRPC has a reduced C_3A (tricalcium aluminate) phase in comparison to OPC. This phase undergoes rapid hydrolysis on mixing with water, therefore the ionic concentrations within the water phase will be different between these cementitious systems. Evidence of this is the resulting increase in resistivity of the fluid phase. The equivalent circuit parameters for the bulk arc are presented in Table IV. In comparison to the equivalent OPC mix (e.g. mix 3), the bulk resistance of SRPC has almost doubled whereas the coefficient of the CPE remains unchanged.

In comparison to mix 3, partial replacement of the OPC with GGBS results in an increase in the impedance. GGBS possesses hydraulic properties although reaction with water is very slow; it could therefore be regarded as inert at this early stage of hydration. Considering the respective contained water phase resistivities, the OPC/GGBS mix shows an increased resistivity in comparison to the respective OPC mix (mix 3). As above, this must indicate a reduction in ionic concentration within the water phase. If it is assumed that GGBS is inert, then it is the OPC within the mix which is contributing to the ionic concentration in the water phase. In comparison to the plain OPC mix, the mass of OPC within mix 6 is halved, and will result in a reduction in a dilution of ionic concentration within the contained water phase. This produces the resulting decrease in ρ_w. The equivalent circuit parameters for the bulk arc are presented in Table IV.

The combination of SRPC/GGBS is as anticipated and results in a further increase in impedance of the system. Once again, consideration should be given to the water-phase resistivity, where this mix is almost three times more resistive than the equivalent plain OPC mix. Equivalent circuit parameters are presented in Table IV.

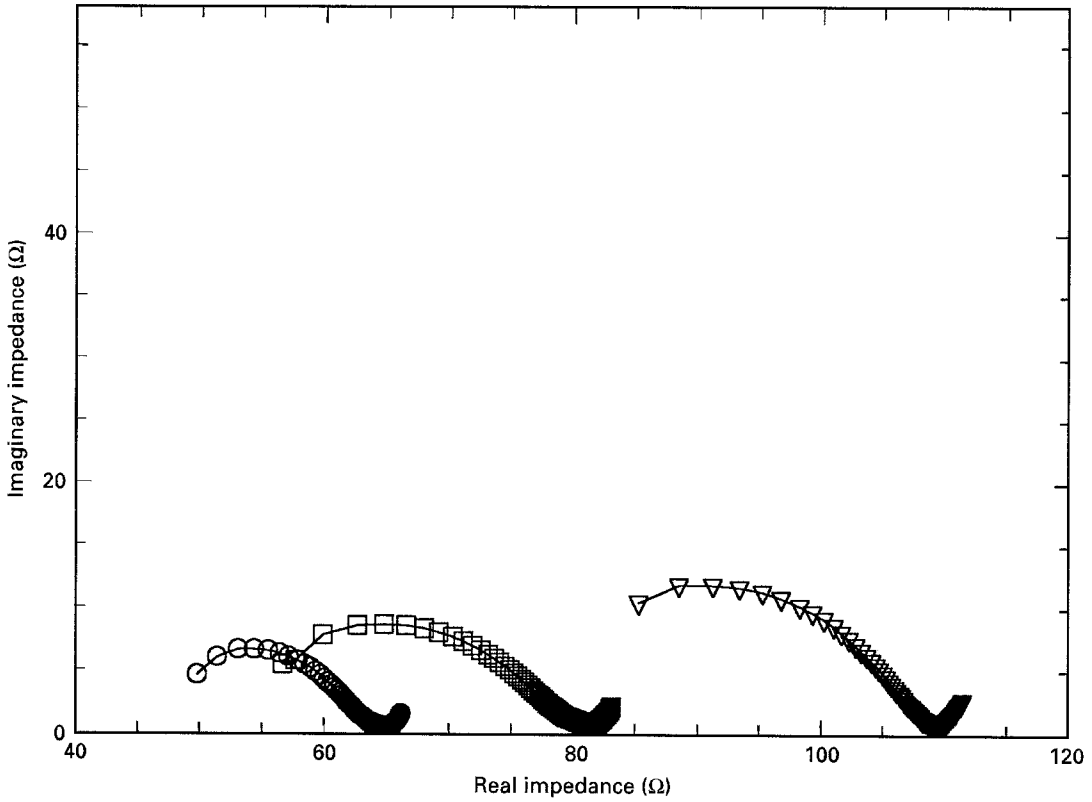

Figure 2 The influence of cementitious binder on impedance response. (▽) Mix 4, (○) Mix 5, (□) Mix 6.

TABLE IV Summary of model parameters for SRPC and GGBS concrete mixes

Mix	R_{bulk} (Ω)	Y_{bulk} (F)	n_{bulk}
4	109	7.16×10^{-8}	0.58
5	64	1.53×10^{-7}	0.56
6	81	4.22×10^{-7}	0.50

Considering Figs 1 and 2, the resistivity of the contained water phase within the concrete mix, which is dependent upon the cementitious binder, would appear to exert a greater influence on the impedance response than variations in water content alone. This is due to the change in ionic concentration within the interstitial water phase.

Fig. 3 presents the response for OPC with partial replacement with PFA. The plots display a unique response which can be divided into two distinct regions: a very flat arc at the low-frequency end of the plot which develops into a more pronounced arc at higher frequencies. The low-frequency arc develops at 300 Hz (for all mixes presented), increasing to a maximum at 8 kHz (for all mixes) and then decreasing to a minimum again (before developing into the second arc). Regarding this minimum value, the frequency at which this occurs varies: 70 kHz for mix 8, 90 kHz for mix 9 and 300 kHz for mix 2 – which is in the order of increasing water content of the mix. Another general observation from the response is the increased impedance of the OPC/PFA mixes in comparison to an equivalent plain OPC mix (e.g. mixes 7 and 9 could be compared); the interstitial water phase of PFA mixes (see Table II) show an increased resistivity when compared to plain OPC mixes. As with the GGBS, the PFA is not contributing in any appreciable degree to the ionic concentration within the water phase.

Unlike GGBS, however, PFA is a true pozzolanic material having no hydraulic properties of its own and requiring calcium hydroxide as an activator. Other features of PFA which should be noted are its distinctive spherical particle shape (although its particle size is similar to OPC) and its lower specific gravity in comparison to OPC (i.e. 2.20 compared with 3.15, respectively). Previous work [22] has shown that the development of the low-frequency arc region is dependent upon the PFA content of the mix. In an effort to explain this impedance behaviour, a proposed circuit model for the response takes the form $(R'_{bulk}Q'_{bulk})(R_{PFA}Q_{PFA})$, where the latter element refers to the response from the PFA particles alone, and the former the response from the OPC/aggregate within the system. For illustrative purposes, Table V presents these elements for mix 9. The CPE associated with the flat arc is several orders of magnitude larger than any of those presented in Tables III or IV. It could be that on gauging with water, an electrical double layer will form around the PFA particle. The charges in this double layer can thereby move more easily over the spherical surface in an alternating field than the OPC of GGBS particles. This gives rise to a double-layer polarization effect. Double-layer effects can induce large dipoles producing large capacitive values; furthermore, double-layer polarization is a low-frequency polarization mechanism, occurring in the range 100 Hz–10 kHz [52–54]. It is interesting to postulate such a mechanism, because PFA concrete develops an arc in this frequency range. Another possible

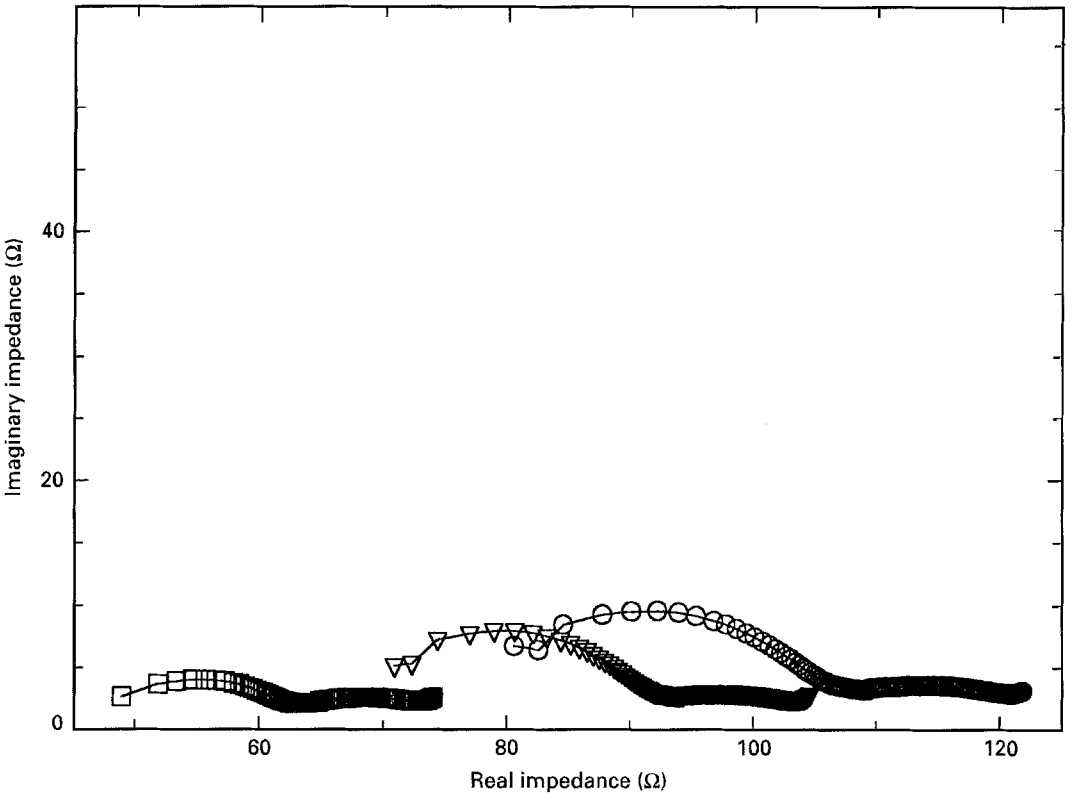

Figure 3 Complex impedance spectra for PFA concretes. (□) Mix 2, (○) Mix 8, (▽) Mix 9.

TABLE V Model parameters for PFA concrete (Mix 8)

R'_{bulk} (Ω)	Y'_{bulk} (F)	n'_{bulk}	R_{PFA}	Y_{PFA}	n_{PFA}
90	1.00×10^{-7}	0.575	20	1.50×10^{-3}	0.35

reason for this flat arc could be due to the ferromagnetic properties of PFA; work is continuing in this respect.

3.3. Additional observations from the data

Additional insights can be obtained by consideration of the bulk resistivity of the concrete mixes together with that of the water phase within the respective mix, as presented in Table III. The bulk resistivity of the sample was obtained directly from the bulk resistance, R_{bulk}, by correcting for sample geometry; for the PFA mixes, this was calculated from $(R'_{bulk} + R_{PFA})$. The simple effective medium equation [18] could be considered

$$\frac{\rho_w}{\rho_{bulk}} = \beta V_f \quad (1)$$

where, in this instance, the ratio ρ_w/ρ_{bulk} represents the normalized resistivity of the mix; V_f is defined as the volume fraction of water in the mix (i.e. water content/1000) and β is a parameter associated with tortuosity and continuity of the conduction paths through the material. β is an empirical constant and, for an ideal parallel arrangement of conductive and non-conductive phases, has the value of unity. This represents an upper bound arrangement for the true

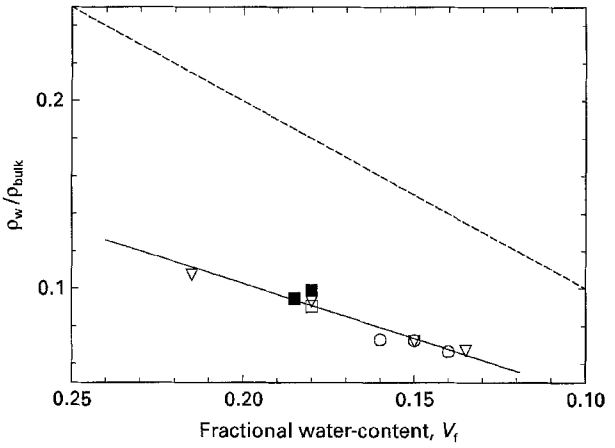

Figure 4 Data for concrete mixes plotted in accordance with Equation 1. β: (– – –) 1, (——) 0.58, (▽) Mixes 1, 3, 7, 10, (○) Mixes 2, 8, 9; (□) Mix 5; (■) Mixes 4 and 6.

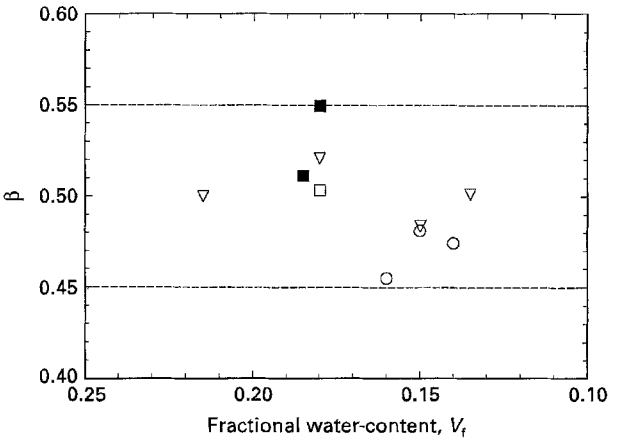

Figure 5 Connectivity parameter, β, versus fractional water content. For key, see Fig. 4.

composite; a lower bound solution would come from a series arrangement where, if the aggregate had infinite resistivity, would produce a value for $\beta = 0$. Fig. 4 presents the data in Table II in the format of Equation 1, with the slope of the line through the data points being 0.58. This indicates a dominance of parallel behaviour and is perfectly plausible at this early stage, and well before setting. For comparison, the curve for $\beta = 1$ is shown on this figure.

Another interesting result comes from a plot of the connectivity parameter, $\beta(= \rho_w/(\rho_{bulk}V_f))$, versus the fractional water content, V_f (Fig. 5). This plot shows that, regardless of water content or cementitious binder, the connectivity parameter falls within a very narrow band: 0.5 ± 0.05. β values for HCP systems are, typically, between one and two orders of magnitude lower than this value [16].

4. Conclusion

Further data have been presented on the complex impedance response of cementitious systems and, unlike much previous work, the study was undertaken on concretes before setting. The data have corroborated and extended a previous study both in the range of mixes tested and analysis and modelling of the impedance spectra. It was shown that there was distortion of the high-frequency bulk arc at frequencies in excess of 4 MHz and was attributed to the inability of nulling procedures completely to eliminate lead effects, etc.

Accepting this limitation, modelling was undertaken using frequencies below this upper limit. Data have been presented on samples which were of realistic size and thus give a true representation of the macroscopic response of the system. In addition to this, mix proportions, water contents, binder contents and binder types were within the range of those used by industry.

The work has also opened up another area for the direct application of impedance spectroscopy techniques, namely as a method for quality control of structural concrete. For example, the unique response of PFA lends the method for, (a) detecting the presence of PFA in a concrete mix, and (b) evaluating the PFA content of the mix and that this complies with specification. Clearly this is of considerable importance to the construction industry in the design of concrete for durability where increasing use is being made of such replacement materials.

Acknowledgements

The author thanks the Engineering and Physical Science Research Council for financial support (Grant GR/J10754) and Mr P. Puyrigaud and the technical staff within the Department for their assistance in the experimental work.

References

1. W. J. McCARTER, S. GARVIN and N. BOUZID, *J. Mater. Sci. Lett.* **7** (1988) 1056.
2. W. J. McCARTER and S. GARVIN, *J. Phys. D Appl. Phys.* **22** (1989) 1773.
3. W. J. McCARTER and R. BROUSSEAU, *Cem. Concr. Res.* **20** (1990) 891.
4. K. BRANTERVIK, A. BERG, G. A. NIKLASSON, B. HEDBERG and L. O. NILSSON, *Europhys. Lett.* **13** (1990) 549.
5. K. BRANTERVIK and G. A. NIKLASSON, *Cem. and Concr. Res.* **21** (1991) 496.
6. A. BERG, G. A. NIKLASSON, K. BRANTERVIK, B. HEDBERG and L. O. NILSSON, *Solid State Commun.* **79** (1991) 93.
7. B. J. CHRISTENSEN, T. O. MASON and H. M. JENNINGS, *J. Am. Ceram, Soc.* **75** (1992) 939.
8. A. BERG, G. A. NIKLASSON, K. BRANTERVIK, B. HEDBERG and L. O. NILSSON, *J. Appl. Phys.* **71** (1992) 5897.
9. P. GU, P. XIE, J. J. BEAUDOIN and R. BROUSSEAU, *Cem. Concr. Res.* **22** (1992) 833.
10. *Idem, ibid.* **23** (1993) 157.
11. P. GU, P. XIE, Z. XU and J. J. BEAUDOIN, *ibid.* **23** (1993) 359.
12. Z. XU, P. GU, P. XIE and J. J. BEAUDOIN, *ibid.* **23** (1993) 531.
13. P. GU, P. XIE and J. J. BEAUDOIN, *ibid.* **23** (1993) 581.
14. *Idem, ibid.* **23** (1993) 853.
15. R. T. COVERDALE, E. J. GARBOCZI, H. M. JENNINGS, B. J. CHRISTENSEN and T. O. MASON, *J. Am. Ceram. Soc.* **76** (1993) 1153.
16. B. J. CHRISTENSEN, R. T. COVERDALE, R. A. OLSEN, S. J. FORDE, E. J. GARBOCZI, H. M. JENNINGS and T. O. MASON, *ibid.* **77** (1994) 2789.
17. R. T. COVERDALE, B. J. CHRISTENSEN, T. O. MASON, H. M. JENNINGS and E. J. GARBOCZI, *J. Mater. Sci.* **29** (1994) 4984.
18. R. T. COVERDALE, B. J. CHRISTENSEN, H. M. JENNINGS, T. O. MASON, D. P. BENTZ and E. J. GARBOCZI, *ibid.* **30** (1995) 712.
19. S. J. FORDE, T. O. MASON, B. J. CHRISTENSEN, R. T. COVERDALE, H. M. JENNINGS and E. J. GARBOCZI, *ibid.* **30** (1995) 1217.
20. W. J. McCARTER, *J. Am. Ceram. Soc.* **78** (1995) 411.
21. C. A. SCUDERI, T. O. MASON and H. M. JENNINGS, *J. Mater. Sci.* **26** (1991) 349.
22. W. J. McCARTER, *Cem. Concr. Res.* **24** (1994) 1097.
23. Y. SCHIMIZU, *Sci. Rep. Tohoku Imperial Univ., First Ser.* **17** (1) (1928) 28.
24. M. G. BAIRE, *Rev. Mater. Construct. Travaux Publics (Paris)* **272** (1932) 182.
25. N. PETIN, M. HIGEROVITSH and E. GOYSINOVICH, *J. Gen. Chem. USSR* **2** (1932) 614.
26. V. A. KIND and V. F. ZHURALER, *Tsement* **5** (9) (1937) 21.
27. J. CALLEJA, *J. Am. Conc. Inst.* **23** (1952) 329.
28. E. HAMMOND and T. D. ROBSON, *The Engineer* **199** (1955) 78.
29. *Idem, ibid.* **199** (1955) 114.
30. H. W. WHITTINGTON, W. J. McCARTER and M. C. FORDE, *Mag. Concr. Res.* **33** (114) (1981) 48.
31. J. B. BARS, J. F. CAMPS and J. DEBUIGNE, *Mater. Construct.* **15** (85) (1982) 33.
32. F. D. TAMAS, *Cem. Concr. Res.* **12** (1) (1982) 115.
33. R. MORELLI, PhD thesis, University of Edinburgh (1985) 179.
34. B. P. HUGHES, A. K. D. SOLEIT and R. W. BRIERLY, *Mag. Concr. Res.* **37** (133) (1985) 243.
35. F. D. TAMAS, M. FARKAS, M. VOROS and D. ROY, in "Proceedings of the 8 th International Congress on Chemistry of Cement", Rio-de-Janeiro, Brazil, 22-27 September, (Alba Gráfica e Editora Ltda.) Vol. VI (1986) pp. 374–80.
36. W. J. McCARTER and A. AFSHAR, *J. Mater. Sci.* **23** (1988) 488.
37. P. GU, Y. FU and J. J. BEAUDOIN, *J. Mater. Sci. Lett.* **12** (1993) 1171.
38. P. GU, V. S. RAMACHANDRAN and J. J. BEAUDOIN, *ibid.* **14** (1995) 503.
39. P. R. CAMP and S. BILOTTA, *J. Appl. Phys.* **66** (1989) 6007.
40. K. OLP, G. OTTO, W. C. CHEW and J. F. YOUNG, *J. Mater. Sci.* **26** (1991) 2978.
41. C. A. HEILAND, "Geophysical Exploration" (New York, Prentice Hall, 1946).

42. G. E. MONFORE, *J. PCA Res. Devel. Labs.* **10** (2) (1968) 35.
43. British Standards Institution BS 12: "Specification for ordinary and rapid hardening Portland cement" (BSI, London, 1978).
44. British Standards Institution BS 4027: "Specification for sulphate resisting Portland cement" (BSI, London, 1980).
45. British Standards Institution BS 3892: "Specification for pulverised fuel ash for use as a cementitious component in structural concrete", (BSI, London, 1982).
46. British Standards Institution BS 6699: "Specification for ground granulated blastfurnace slag for use with Portland cement" (BSI, London, 1985).
47. British Standards Institution BS 882: "Specification for aggregates from natural sources for concrete" (BSI, London, 1983).
48. D. C. TEYCHENNE, J. C. NICHOLLS, R. E. FRANKLIN, R. E. HOBBS and H. C. ERNTROY, "Design of normal concrete mixes" (Department of the Environment, HMSO, London 1975), pp 11–21.
49. British Standards Institution BS 1881: Part 116: "Method for determination of compressive strength of concrete cubes" (BSI, London, 1983).
50. British Standards Institution BS 1881: Part 108: "Method for making test cubes from fresh concrete" (BSI, London, 1983).
51. B. A. BOUKAMP, "Equivalent Circuit: EQUIVCRT.PAS", University of Twente, Department of Chemical Technology, P.O. Box 217, 7500 AE Enschede, The Netherlands (1989).
52. H. P. SCHWAN, G. SCHWARZ, J. MACZUK and H. PAULY, *J. Phys. Chem.* **66** (1962) 2626.
53. G. SCHWARZ, *ibid.* **66** (1962) 2636.
54. J. B. HASTED, "Aqueous Dielectrics" (Chapman and Hall, London, 1973).

Received 1 May 1995
and accepted 13 February 1996